

Performance analysis of coherent optical communication based on hybrid algorithm

Wei Liu^a, Dairan Jin^a, Wenxiao Shi^a, Jingtai Cao^{a,b,*}

^a College of Communication Engineering, Jilin University, 5372 Nanhu Road, Changchun 130012, PR China

^b Changchun Institute of Optics, Fine Mechanics and Physics, Chinese Academy of Sciences, 3888 Nanhu Road, Changchun 130033, PR China

ARTICLE INFO

Keywords:

Adaptive optics
Bit error rate
Mixing efficiency
Signal-to-noise ratio
Free-space optical communication
Binary Phase Shift Keying

ABSTRACT

The performance of coherent free-space optical communication (FSOC) is often affected by atmospheric turbulence. Sensorless adaptive optics are widely used in coherent FSOC to mitigate the effect of atmospheric turbulence. However, the control algorithm for sensorless adaptive optics systems remains weak. To enhance the various performance indicators of coherent FSOC, we propose a hybrid algorithm to improve the coupling efficiency and mixing efficiency (ME) of the system while reducing the bit error rate (BER). This algorithm combines the fast convergence rate of the simulated annealing (SA) algorithm at the initial cooling stage and the beneficial convergence effect of the stochastic parallel gradient descent (SPGD) algorithm, avoiding the algorithm's need for more iterations and its tendency to enter local optimisation. The simulation results show that the performance of the proposed hybrid algorithm outperforms that of the traditional SPGD algorithm, regardless of the intensity of the atmospheric turbulence. The SA and hybrid algorithms display similar performances in strong atmospheric turbulence, while the hybrid algorithm shows better performance than that of the SA algorithm in weak atmospheric turbulence.

1. Introduction

With higher transmission rates, higher channel utilisation, and other advantages, FSOC is currently considered an important supplement to traditional wireless communication and fibre optics communication systems [1]. In particular, coherent FSOC has advantages in intensity modulation direct detection systems, such as high spectrum efficiency and flexibility for advanced modulation formats and great sensitivity in homodyne detection. For communication performance, the homodyne detection module in coherent FSOC effectively improves the sensitivity compared to heterodyne detection [2]. However, its development is restricted by atmospheric turbulence. The performance of a coherent FSOC is influenced by the random phase disturbance caused by the random fluctuation of turbulence. Adaptive optics (AO) systems are considered an effective way to solve this problem [3]. A 97-element continuous surface deformable mirror is used to correct wavefront aberrations, and the ME and BER under different conditions are analysed [4]. Additionally, a new cost function for the wavefront reconstruction problem with a Shack–Hartmann wavefront sensor has been established. It addresses the disadvantage of least square reconstruction of the wavefront by providing smooth transitions of branch cut creation,

evolution, and disappearance. Experimental results show that it could be used as a better method for handling wavefront aberrations due to strong turbulence [5]. A multi-frame Shack–Hartmann wavefront sensor (WFS) measurement improved the accuracy of the reconstructed wavefront. The results showed that the method is robust in terms of coping with velocity estimation errors [6]. Considering the effect of the greenwood frequency, which severely impact the BER of FSOC [7], an experiment verified that the temporal characteristics may be stronger than the spatial characteristics of atmospheric turbulence [4]. The traditional wavefront correction method adopts a closed-loop negative feedback working mode; however, wave-front phase conjugation was used to correct the optical wave signal to meet the standard before transmission.

Wavefront-less AO systems have been increasingly attached, because a beam split is not required; therefore, they are not sensitive to light intensity flickers. The SA algorithm increased the average coupling efficiency in the FSOC system, and it was proven to be better than SPGD algorithm in some situations. However, the BER and ME in coherent systems have not yet been analysed [8]. When more Zernike modes are corrected, the performances of a system operating in non-Kolmogorov turbulence strongly increase [9]. Regarding machine learning, which

* Corresponding author at: College of Communication Engineering, Jilin University, 5372 Nanhu Road, Changchun 130012, PR China.

E-mail address: jingtai1985@163.com (J. Cao).

<https://doi.org/10.1016/j.optlastec.2022.107878>

Received 3 August 2021; Received in revised form 6 December 2021; Accepted 10 January 2022

Available online 17 January 2022

0030-3992/© 2022 Elsevier Ltd. All rights reserved.

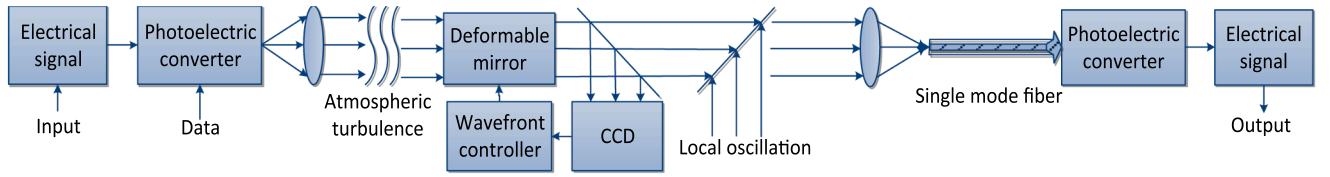


Fig. 1. Coherent FSOC system.

can categorise and predict wavefront aberrations, signal impairments in optical networks have been analysed, and the results showed the relationship between signal-to-noise ratio (SNR) and transmission speeds [3]. The directivity error of coherent FSOC in a turbulent channel was analysed in detail by H. J. et al. [10]; however, among the performance metrics, simple BER analysis is not convincing enough on the performance of the system. The hybrid algorithm is widely used to replace the wavefront sensor of the AO system in an FSOC. CNN (Convolutional Neural Networks) is an artificial intelligence algorithm, which has attracted much attention for its strong performance and flexibility. CNN and SPGD algorithm are used together in [1] to improve the coupling efficiency and Strehl ratio (SR) under atmospheric turbulence, where the CNN model roughly classifies and corrects the aberrations, and the SPGD algorithm fine-tunes aberrations. However, the accuracy rate of this hybrid algorithm decreased significantly when the categories were large [11]. The traditional Hartmann–Shack sensor scatters the light while occupying a large amount of space in the system; hence, it is not suitable for all applications. Thus, the wavefront-less AO algorithm has a unique advantage in FSOC [12]. To increase the convergence rate, wavefront-less AO algorithms based on incoherent FSOC systems were investigated in our previous work [13]. However, little research has been conducted on the performance of the sensorless AO algorithm based on a coherent FSOC system.

In this paper, a hybrid algorithm is proposed to increase the performance indicators of a coherent communication system. In the proposed hybrid algorithm, the convergence rate is increased by the rapid cooling process of the SA [14] algorithm in coarse correction, whereas the performance index is guaranteed by the SPGD algorithm [15] in fine correction. We investigated different performance indices such as BER, ME, and coupling efficiency. According to the simulation results, the hybrid algorithm can reduce the calculation amount while improving the performance of the system. The hybrid algorithm can achieve better performance by using fewer iterations than the other two algorithms in atmospheric turbulence of different intensities [16]. The results of this study can provide a reference for the design of coherent optical communication systems.

2. System model

The system model of the coherent FSOC with a closed-loop controlled AO is shown in Fig. 1. The digital signal is transformed to a light signal by the photoelectric converter before transmission. Then, the laser beam disturbed by atmospheric turbulence is corrected using wireless adaptive optics (WLAO) [17]. After the corrected laser beam is mixed with the local oscillation (LO) laser beam, the mixed laser beam is coupled into a single-mode fibre. The mixed laser beam is then transformed into a digital signal. During this process, the laser beam is disturbed by atmospheric turbulence, and the amplitude and phase of the laser beam is changed; thus, WLAO is introduced to correct the distortion. The WLAO work cycle was divided into three steps. First, the charge coupled device (CCD) obtains the distortion information of the laser beam, then the wavefront controller controls the deformable mirror (DM) [18] based on the distortion information, and the adaptive DM can correct the light wave in real time [19]. Thus, communication performance is improved.

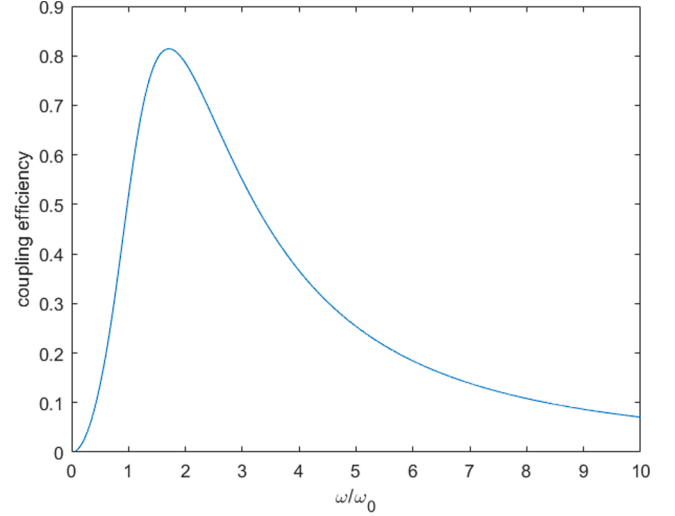


Fig. 2. Change curve of coupling efficiency.

3. Theoretical basis

3.1. Coupling efficiency analysis

In free-space optical communication, light needs to be coupled into a single-mode fibre for complete transmission. Therefore, researchers typically use coupling efficiency when analysing the quality of free-space optical communications. However, the alignment problem occurs in the coupling process owing to various wavefront aberrations introduced by atmospheric turbulence [20], which results in a decrease in the coupling efficiency. To solve this problem, we can correct the wavefront aberration using various adaptive algorithms. In the ideal state, the coupling principle of the optical fibre is similar to the pattern matching relation between the airy mode field and optical fibre mode field, and the distribution of the diffraction field and the incident light wave mode field also satisfies the Fourier transform.

The coupling efficiency [21] of the fibre is defined as the ratio of the optical power coupled into the fibre to the incident optical power of the aperture of the receiving antenna, which can be expressed as (1):

$$\eta_c = \frac{P_c}{P_a} = \frac{|\int_A U_i(r) \cdot U_m^*(r) dr|^2}{\int_A |U_i(r)|^2 dr} \quad (1)$$

Here, P_c is the power of the light coupled into the fibre, P_a is the power of the incident light, and $U_i(r)$ is the incident light wave mode field of the receiving antenna [21], which can be expressed as:

$$U_i(r) = \frac{\pi D_R^2}{4\lambda f} \left[2 \frac{I_1(3.83r/\omega)}{(3.83r/\omega)} \right] \quad (2)$$

Here, λ is the wavelength of the laser, f is the focal length, $I_1()$ is the Bessel function of the first-order modified, r is the distance in polar coordinates, D_R is the lens aperture, and ω is the mode radius of the Airy disk.

$U_m(r)$ is the optical fibre mode field [22], which can be expressed as Equation (3):

$$U_m(r) = \sqrt{\frac{2}{\pi\omega_0}} \exp\left(-\frac{r^2}{\omega_0^2}\right) \quad (3)$$

where ω_0 is the mode radius of the single-mode fibre.

This can be obtained by combining equations (2) and (3) to obtain:

$$\eta_c = 2\pi \exp\left(\frac{-3.667}{(\omega/\omega_0)^2}\right) \times I_{1/2}^2\left(\frac{1.834}{(\omega/\omega_0)^2}\right) \quad (4)$$

where $I_{1/2}()$ is a modified Bessel function of half order.

Using ω/ω_0 as an independent variable and coupling efficiency as a dependent variable, we can obtain Fig. 2.

Fig. 2 shows that the maximum coupling efficiency of the fibre is approximately 0.81. The expression of the coupling efficiency under adaptive optics correction [23] is:

$$\eta_c = 8a^2 \int_0^1 \int_0^1 \exp[-(a^2 + A_R/A_C)(x_1^2 + x_2^2)] \cdot I_0(2A_R/A_C x_1 x_2) x_1 x_2 dx_1 dx_2 \quad (5)$$

a is the aperture radius of receiving lens, and it can be expressed as:

$$a = \frac{D_R \pi \omega_0}{2 \lambda f} \quad (6)$$

A_R is the cross-sectional area of the receiving aperture, which is defined as:

$$A_R = \frac{\pi D_R^2}{4} \quad (7)$$

A_C is the coherent area of incident light space, which is defined as:

$$A_C = \pi \rho_C^2 \quad (8)$$

ρ_C is the standard spatial coherence length corrected by the fried function [24] and can be expressed as:

$$\rho_C = 0.286 \left(\frac{3.44}{coef(j)}\right)^{0.6} j^{-0.362} r_0 \quad (9)$$

where j is the number of Zernike coefficients corrected.

3.2. ME analysis

We assumed a plane wave as the LO, and the intensity of the optical signal (OS) was uniform. When the frequency of the LO is equal to that of the OS, it can be called homodyne detection. If the frequency of LO is not equal to that of the OS, it can be called heterodyne detection.

In homodyne detection, the ME [7] can be defined by:

$$\eta_{\infty SR} = \frac{\int \int A_S A_O \cos(\phi(r) + \phi(t)) ds^2}{\int A_S^2 ds \int A_O^2 ds} \quad (10)$$

where A_S and A_O are the amplitudes of the OS and LO in the coherent FSO system, respectively. $\phi(r)$ is a time-independent phase variable introduced by atmospheric turbulence, and $\phi(t)$ is a space coordinate-independent variable related to the modulation phase of the OS.

3.3. BER analysis

BER is an important parameter for evaluating transmission performance. This parameter is often significantly affected by the atmospheric turbulence. The beam deviation caused by turbulence will bring an additional SNR ratio and eventually lead to a decline in communication reliability.

The BER of the coherent FSO system [8] can be obtained using equation (11), as follows:

$$BER = \frac{1}{2} \operatorname{erfc}\left(\sqrt{\frac{SNR}{2}}\right) \quad (11)$$

where SNR is the signal-to-noise ratio of the coherent FSO, and erfc is the complementary. The SNR can be expressed by the quantum efficiency, the number of photons received within a single bit, and ME [8]. For a Binary Phase Shift Keying (BPSK) received system disturbed by atmospheric turbulence, the BER is:

$$BER = \frac{1}{2} \operatorname{erfc}\left(\sqrt{2\delta N_p \eta}\right) \quad (12)$$

where δ is the quantum efficiency of the detector, η is ME, and N_p is the number of photons received within a single bit.

4. Analysis of several WLAO algorithms

4.1. Simulated annealing algorithm

The simulated annealing algorithm is a physical annealing model-based algorithm used to find the lowest energy state. This algorithm simulates the process by which particles gradually change into an ordered state as an object cools down at a high temperature. In the process of change, it maintains the equilibrium state as much as possible and reaches the ground state at room temperature. This algorithm is suitable for any process that requires a global search. It uses a high initial temperature to increase the number of iterations to obtain the lowest energy solution. In this process, generating a new solution must be repeated, the difference in the objective function is calculated, and a new solution is chosen. According to the metropolis criteria, if the energy of the new solution is lower than that of the original solution, the new solution is accepted. Otherwise, the new solution is received with a probability of $\exp(-\Delta T/T)$. Because its convergence speed is faster than that of the SPGD algorithm, this algorithm is used for coarse correction to ensure the real-time performance of the system.

The specific algorithm flow is as follows:

- (1) Set the initial value of the Cooling Schedule.
- (2) Generate new solution S.
- (3) Calculate the incremental ΔT .
- (4) For $\Delta T < 0$, accept the new solution, for $\Delta T > 0$, accept the new solution with a probability of $\exp(-\Delta T/T)$.
- (5) Perform the appropriate number of steps 2 through 4 according to the number of iterations set by the Cooling Schedule.
- (6) Attenuate T, go to step 2, and repeat until $T = 0$.

4.2. Stochastic parallel gradient descent algorithm

The SPGD algorithm is a typical sensorless correction algorithm. It has attracted a significant amount of attention because it is particularly suitable for correcting wavefront aberrations caused by atmospheric turbulence that cannot be accurately described by a specific model.

The SPGD algorithm uses the image quality evaluation function J to search for the optimal correction voltage in the gradient descent direction. J can be expressed as the SR. The image quality evaluation algorithm calculates the ratio of the actual light intensity to the ideal optimal light intensity in the unit circle. Generally, when the image quality evaluation reaches 0.8, the wavefront is considered well-corrected. Its specific algorithm [25] analyses the image quality of the initial distorted wavefront, and the quality value J can be obtained using Equations (13), (14), and (15).

$$J_+^{(n)} = J[u^{(n)} + \delta u^{(n)}] \quad (13)$$

$$J_-^{(n)} = J[u^{(n)} - \delta u^{(n)}] \quad (14)$$

$$\delta J^{(n)} = J_+^{(n)} - J_-^{(n)} \quad (15)$$

The updated iterative voltage is calculated through the expression,

$$u^{(n+1)} = u^{(n)} + p \delta J^{(n)} \delta u^{(n)} \quad (16)$$

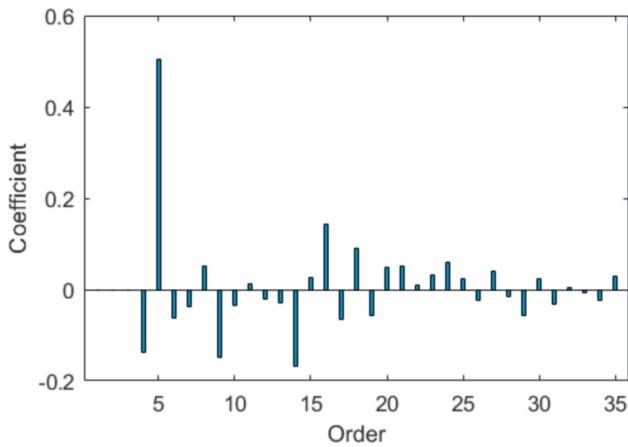


Fig. 3. Zernike coefficients of initial distortion in weak turbulence.

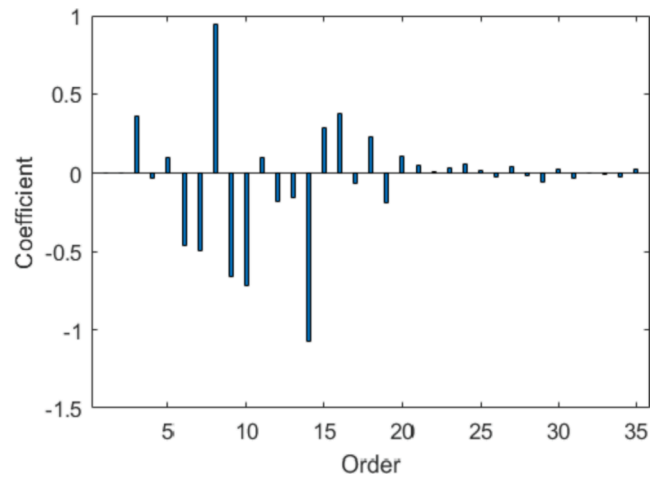


Fig. 4. Zernike coefficients of initial distortion in strong turbulence.

where p is the gain coefficient.

Via this process, we can calculate an updated J through iterative operations until the index reaches the standard. After many iterations, the SR approaches the lowest value with the number of iterations.

The specific algorithm flow is as follows:

- (1) Send wavefront aberration to the image quality analyser.
- (2) Set the initial value of the disturbance voltage.
- (3) Randomly generate a disturbance matrix.
- (4) Obtain image quality analysis of the forward and reverse disturbances.
- (5) The iterative voltage is generated.
- (6) The above steps are repeated until the terminal conditions are met.

4.3. Hybrid algorithm

Among the current fast correction algorithms, convolution neural network algorithms are only suitable for wavefront aberrations described by lower-order Zernike coefficients. In the actual transmission process, the 35 order Zernike polynomial can perfectly represent wavefront aberrations. In this situation, too many samples are required to deal with complex turbulence, making its classification difficult and impractical.

The advantage of the SA algorithm is that it has a fast convergence speed. However, the effect of the SA algorithm is related to the parameter setting; thus, it cannot guarantee that every correction result is accurate. The advantage of the SPGD algorithm is its universality and maturity, but the disadvantage is that it is slower and may enter local optimisation, the probability of which depends on the peak valley value.

To address these issues, a hybrid algorithm is proposed herein. First, the SA algorithm is used to correct aberrations until the Root Mean Square (RMS) is reduced to a certain degree. Then, the residual aberrations can be corrected using the SPGD algorithm. Theoretically, the SA algorithm has a very fast convergence speed for coarse correction. In order to reduce the wavefront aberration quickly, we first use the SA algorithm to make a coarse correction. At the same time, the peak valley (PV) value of the aberration is greatly reduced after SA algorithm correction; thus, when the SPGD algorithm is used to correct the residual error, the possibility of entering the local optimisation process will be greatly reduced. Thus, the real-time accuracy of the system is guaranteed.

5. Numerical simulation

To verify the performance of these algorithms, we used two sets of different Zernike coefficients to fit the initial aberrations due to strong and weak turbulence. The Zernike coefficient can represent the wave-

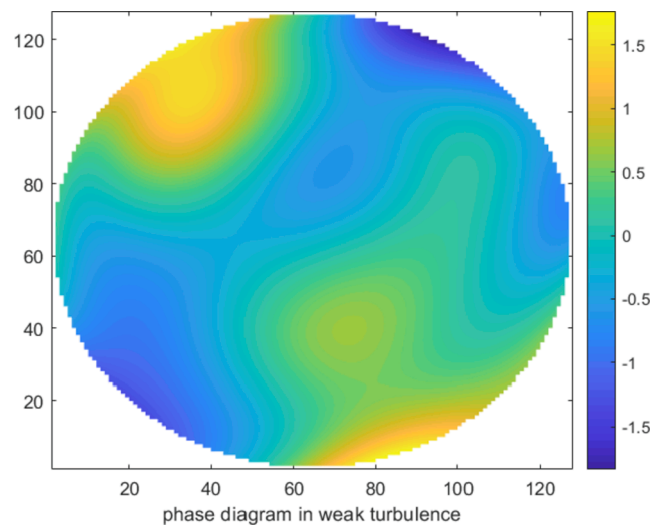


Fig. 5. Phase diagrams for weak turbulence.

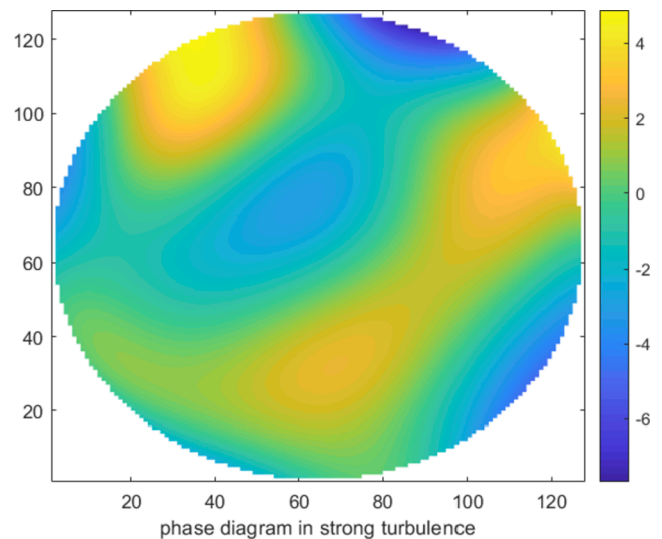


Fig. 6. Phase diagrams for strong turbulence.

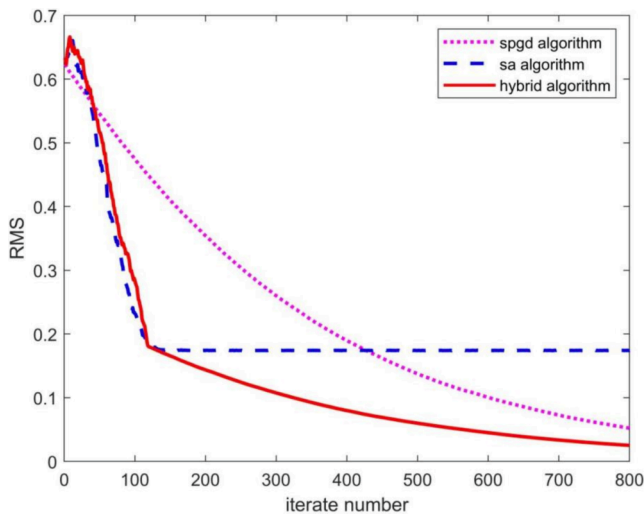


Fig. 7. Changes of RMS with the number of iterations for weak turbulence.

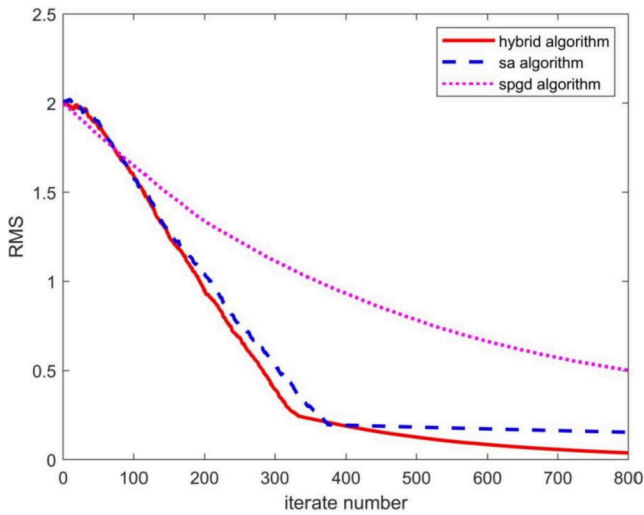


Fig. 8. Changes of RMS with the number of iterations for strong turbulence.

front aberration intensity; the larger the value, the larger the corresponding aberration. We assume a laser beam with a wavelength of 1.55 μm and that the ratio of the optical lens diameter to the focal length is 1. In this system, the number of photons received within a single bit is 10, the mode radius of the Airy disk is 10^{-12} , the quantum efficiency of the detector is 1. Two wavefront aberrations that meet the above conditions are randomly generated, and their Zernike coefficients are shown in Figs. 3 and 4.

The corresponding phase diagrams are given in Figs. 5 and 6.

The SPGD algorithm, SA algorithm, and hybrid algorithm were used for the above two aberrations. The RMS changes after 800 iterations are shown in Figs. 7 and 8.

According to Fig. 9, the effect of the first 400 iterations is relatively obvious. After 600 iterations, the image has converged and the phase is basically restored, thereby far-field spots can be concentrated, which proves the effectiveness of the hybrid algorithm.

The coupling efficiency for different intensities of turbulence after 800 iterations is shown in Figs. 10 and 11.

The ME for different intensities of turbulence after 800 iterations is shown in Figs. 12 and 13.

The BER for different intensities of turbulence after 800 iterations is displayed in Figs. 14 and 15.

According to the Fig. 7, it can be found that in the case of weak

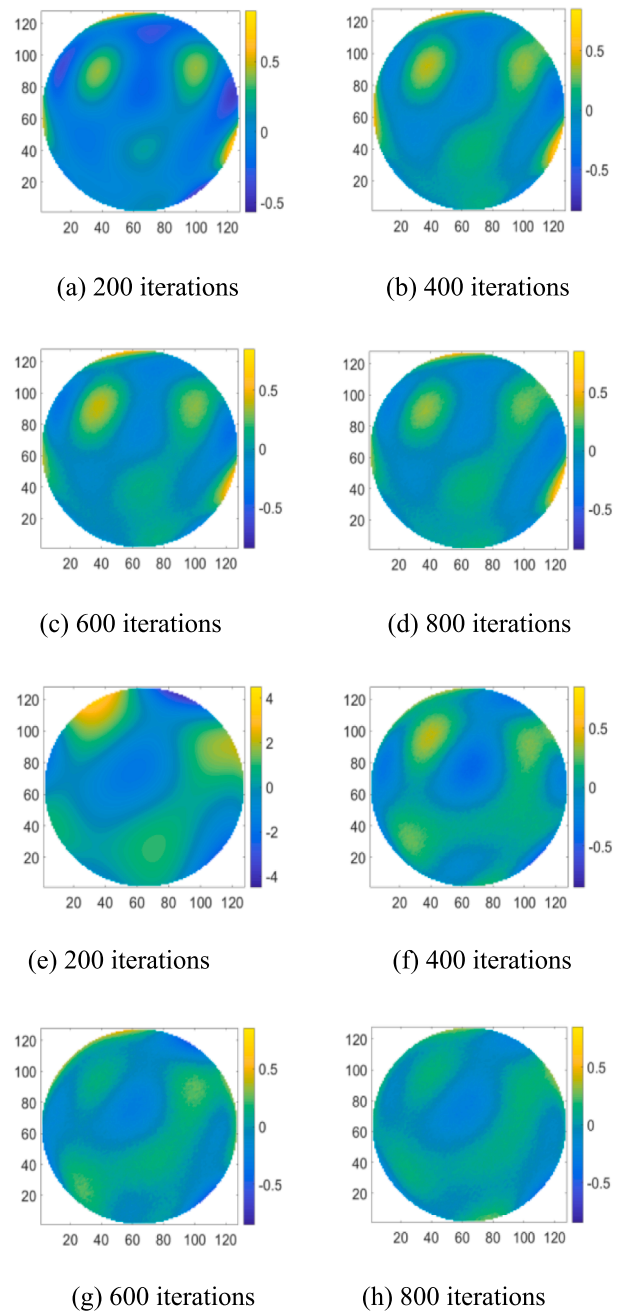


Fig. 9. Change of wave-front images with the number of iterations for weak and strong turbulence. (a)-(d) for weak turbulence and (e)-(h) for strong turbulence.

turbulence, the SA algorithm and hybrid algorithm can reduce RMS to 0.15 after 150 iterations, whereas the SPGD algorithm needs 500 iterations to achieve similar results. Therefore, compared with the efficiency of the SPGD algorithm, the efficiencies of the other algorithms are improved by 70%. After 800 iterations, the RMS of the hybrid algorithm is 0.03 and the coupling efficiency is 0.80; the RMS of the SPGD algorithm is 0.05 and the coupling efficiency is 0.80; the RMS of the SA algorithm is 0.18 and the coupling efficiency is 0.78. The SPGD algorithm after 800 iterations is superior to the SA algorithm, but its result is not as good as that of the hybrid algorithm. In the case of strong turbulence, after 800 iterations, the RMS of the hybrid algorithm is 0.03 and the coupling efficiency is 0.80; the RMS of the SPGD algorithm is 0.5 and the coupling efficiency is 0.78; the RMS of the SA algorithm is 0.15 and the coupling efficiency is 0.80. Under strong turbulence, the SPGD

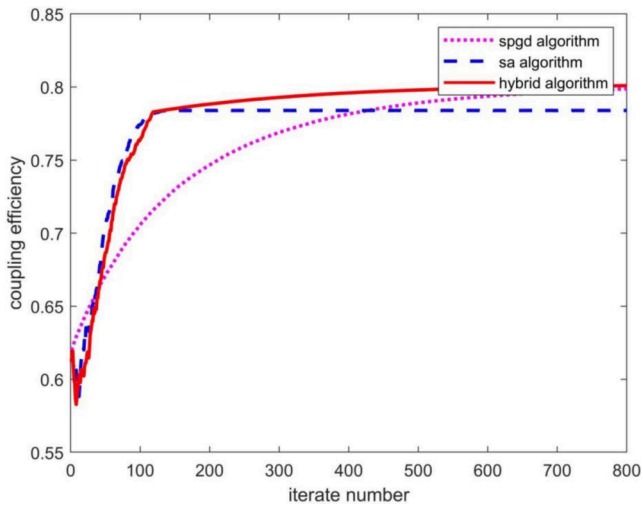


Fig. 10. Changes of coupling efficiency with the number of iterations for weak turbulence.

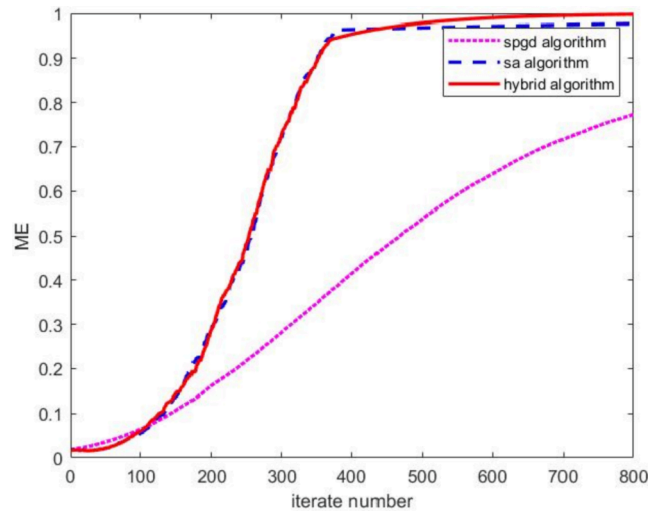


Fig. 13. Changes of ME with the number of iterations for strong turbulence.

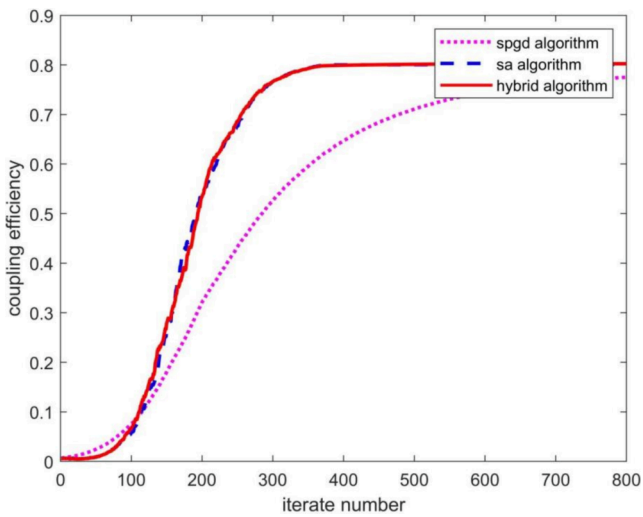


Fig. 11. Changes of coupling efficiency with the number of iterations for strong turbulence.

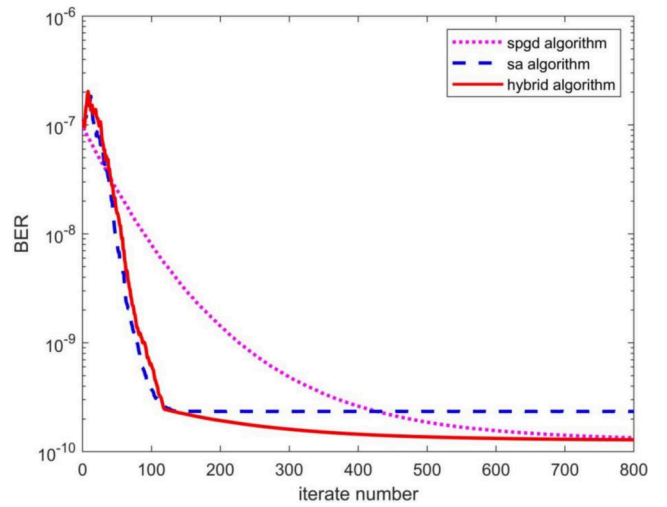


Fig. 14. Changes of BER with the number of iterations for weak turbulence.

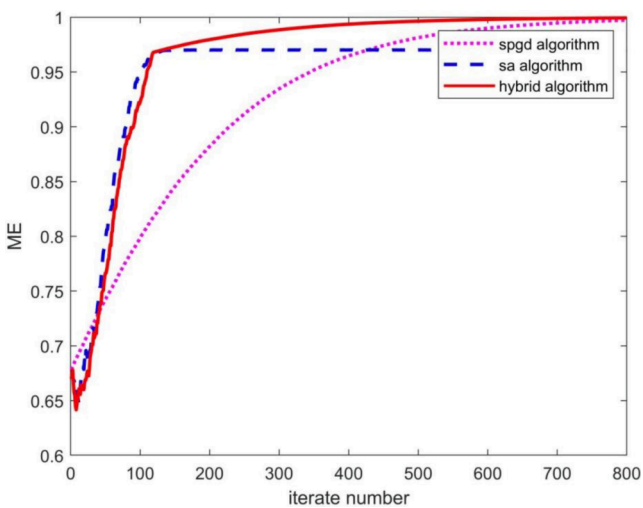


Fig. 12. Changes of ME with the number of iterations for weak turbulence.

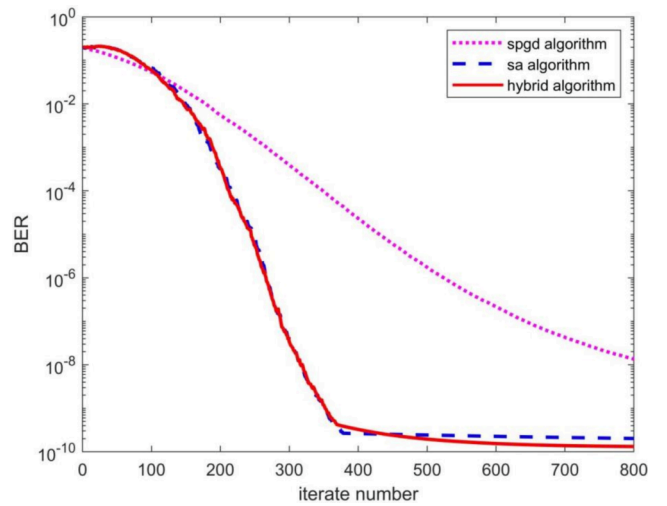


Fig. 15. Changes of BER with the number of iterations for strong turbulence.

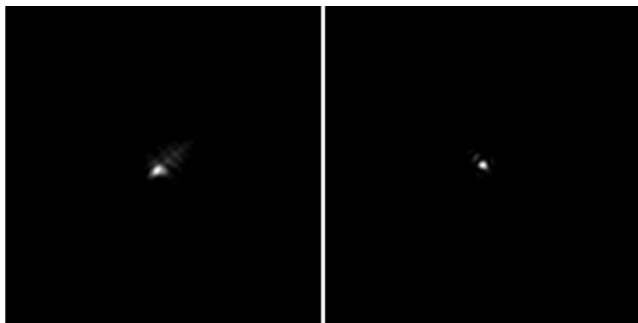


Fig. 16. Far-field images before and after correction for weak turbulence.

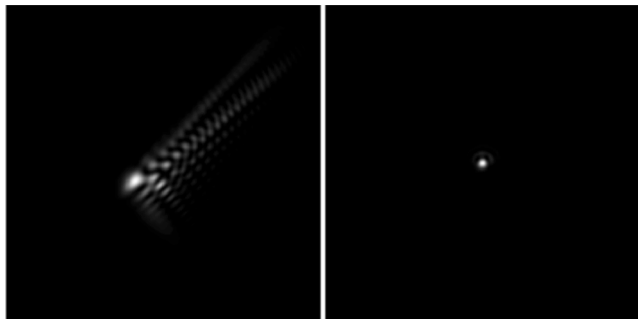


Fig. 17. Far-field images before and after correction for strong turbulence.

algorithm performs poorly, but the hybrid algorithm and SA algorithm perform significantly better, with the hybrid algorithm slightly outperforming the SA algorithm after 400 iterations. As for ME, the result shows that after several iterations, the ME may approach 1, leading to a rapid decline in the BER. This phenomenon was more pronounced under weak turbulence.

Among the existing hybrid algorithms, the algorithm proposed in reference 10 achieves an effective rough classification with CNN, followed by fine correction using the SPGD algorithm. RMS reduces to 0.3785 after the CNN module, and RMS converges to 0.216 after 200 iterations of the SPGD algorithm. Although the hybrid algorithm proposed in this paper lacks the CNN classification process, the rapid convergence effect of the SA algorithm in rough correction can cause RMS to decrease significantly. After 120 iterations, RMS may be reduced to 0.179 in this paper. In contrast to the algorithm in reference 10, this hybrid algorithm can keep lowering the RMS. Finally, the RMS has been reduced to 0.03.

In theory, the hybrid algorithm based on the SPGD algorithm and the Newton iterative algorithm [12] has a good fitting effect, but it requires to adjust the gain coefficient depending on the situation to get the optimal convergence effect. The hybrid algorithm in reference 10 got the RMS of 0.1149. However, the hybrid algorithm in this paper can produce a similar result in less than 300 iterations and has a good effect in following iterations, therefore it has benefits.

According to the simulation results, the hybrid algorithm is superior in the case of both weak and strong turbulence. The hybrid algorithm has the advantage of quickly correcting the aberrations caused by turbulence of various intensities, giving it greater adaptive correction. Figs. 16 and 17 show the far-field images before and after correction for weak and strong turbulence.

6. Conclusion

The control algorithm has a significant influence on the quality of the coherent FSO. In this study, the SA and SPGD algorithms were combined to form a hybrid algorithm. This hybrid algorithm makes full use

of the fast convergence speed in the coarse correction of the SA algorithm and uses the SPGD algorithm to correct the residual error. This reduces the possibility of local optimisation in the traditional SPGD algorithm and ensures the reliability of the correction results. The simulation results show that the hybrid algorithm can significantly reduce the number of iterations in turbulent environments with different intensities, while improving the performance indicators of the coherent FSO.

Formatting of funding sources

This work was supported by the National Natural Science Foundation of China (Grant Nos. 62001448 and U21A20451).

CRediT authorship contribution statement

Wei Liu: Conceptualization. **Dairan Jin:** Data curation. **Wenxiao Shi:** Supervision. **Jingtai Cao:** Software, Methodology.

Declaration of Competing Interest

The authors declare that they have no known competing financial interests or personal relationships that could have appeared to influence the work reported in this paper.

References

- [1] Z.K. Li, X.H. Zhao, BP artificial neural network based wave front correction for sensor-less free space optics communication, *Opt. Commun.* 385 (2017) 219–228.
- [2] C. Liu, M. Chen, S. Chen, H. Xian, Adaptive optics for the free-space coherent optical communications, *Opt. Commun.* 361 (2016) 21–24.
- [3] Y.i. Wang, L. Zhu, W. Feng, Performance study of wavelength diversity serial relay OFDM FSO system over exponentiated Weibull channels, *Opt. Commun.* 478 (2021) 126470, <https://doi.org/10.1016/j.optcom.2020.126470>.
- [4] Z. Li, J. Cao, X. Zhao, W. Liu, Combinational-deformable-mirror adaptive optics system for atmospheric compensation in free space communication, *Opt. Commun.* 320 (2014) 162–168.
- [5] A. Kobayashi, H. Kawashima, N. Saito, M. Momiuchi, A. Koga, R. Furukawa, K. Masunishi, Ieee, Novel adaptive optics system with an electrostatically-driven deformable mirror and wavefront compensation algorithm, 2007.
- [6] C. Niu, X.e. Han, Improved Artificial Bee Colony algorithm for wavefront sensor-less system in Free Space Optical communication, in: Y. Liao, W. Zhang, D. Jiang, W. Wang, G. Brambilla (Eds.), *Aopc 2015: Optical Fiber Sensors and Applications*, 2015.
- [7] J. Cao, X. Zhao, W. Liu, H. Gu, Performance analysis of a coherent free space optical communication system based on experiment, *Opt Express.* 25 (13) (2017 Jun 26) 15299–15312, <https://doi.org/10.1364/OE.25.015299>. PMID: 28788957.
- [8] W. Liu, K. Yao, D. Huang, X. Lin, L. Wang, Y. Lv, Performance evaluation of coherent free space optical communications with a double-stage fast-steering-mirror adaptive optics system depending on the Greenwood frequency, *Opt. Express* 24 (2016) 13288–13302.
- [9] H. Ma, C. Fan, P. Zhang, J. Zhang, C. Qiao, H. Wang, Adaptive optics correction based on stochastic parallel gradient descent technique under various atmospheric scintillation conditions: numerical simulation, *Applied Physics B-Lasers and Optics* 106 (4) (2012) 939–944.
- [10] H. Gu, M. Liu, H. Liu, X. Yang, W. Liu, An algorithm combining convolutional neural networks with SPGD for SLAO in FSO, *Opt. Commun.* 475 (2020) 126243, <https://doi.org/10.1016/j.optcom.2020.126243>.
- [11] L. Zuo, Y. Ren, A. Dang, H. Guo, Ieee, Performance of Coherent BPSK Systems using Phase Compensation and Diversity Techniques, 2010 Ieee Global Telecommunications Conference Globecom 20102010.
- [12] Y.u. Zhang, X. Tian, R. Liang, SPGD and Newton iteration mixed algorithm used in freeform surface metrology, *Opt. Lasers Eng.* 129 (2020) 106050, <https://doi.org/10.1016/j.optlaseng.2020.106050>.
- [13] Z.K. Li, J.T. Cao, X.H. Zhao, W. Liu, Atmospheric compensation in free space optical communication with simulated annealing algorithm, *Opt. Commun.* 338 (2015) 11–21.
- [14] G.-M. Dai, V.N. Mahajan, Zernike annular polynomials and atmospheric turbulence, *J. Opt. Soc. Am. A-Opt. Image Sci. Vis.* 24 (2007) 139–155.
- [15] J. Cao, X. Zhao, Z. Li, W. Liu, H. Gu, Modified artificial fish school algorithm for free space optical communication with sensor-less adaptive optics system, *J. Korean Phys. Soc.* 71 (2017) 636–646.
- [16] A.Y. Shikhovtsev, P.G. Kovadlo, Optical turbulence and different parameters of airflow, 2014.
- [17] J.-M. Kang, P. Guo, Y.-C. Zhang, H. Chen, S.-Y. Chen, X.-Y. Ge, Analysis of optimum coupling efficiency between random light and single-mode fiber, in: Y. Rao (Ed.), *International Symposium on Photoelectronic Detection and Imaging 2013: Fiber Optic Sensors and Optical Coherence Tomography*, 2013.

- [18] T. Liu, W. Xie, L. Yang, J. Zhu, Q. Ling, Wave-front Aberration Modeling based on Wavelet Methods, 2014 33rd Chinese Control Conference 2014, pp. 7388–7392.
- [19] X.-I. Yin, J.-L. Lin, H. Chang, X.-z. Cui, Y.-L. Guo, H.-Y. Liao, C.-Y. Gao, G.-h. Wu, G.-Y. Liu, J.-K. Jiang, Q.-H. Tian, A new version of Stochastic-parallel-gradient-descent algorithm (SPGD) for phase correction of a distorted orbital angular momentum (OAM) beam, in: J. Guofan, Z. Guangjun (Eds.) Fourth Seminar on Novel Optoelectronic Detection Technology and Application, 2018.
- [20] M. Yu, M.A. Vorontsov, Bandwidth estimation for adaptive optical systems based on stochastic parallel gradient descent optimization, in: J.D. Gonglewski, M.T. Gruneisen, M.K. Giles (Eds.) Advanced Wavefront Control: Methods, Devices, and Applications II 2004, pp. 189–199.
- [21] B. Cao, P. Jiang, H. Yang, Y. Qin, M. Zhou, Coupling system with concave and positive-negative angular cone lenses group for the Cassegrain receiving antenna system, *Opt. Commun.* 493 (2021) 127029, <https://doi.org/10.1016/j.optcom.2021.127029>.
- [22] Y.K. Liu, J.L. Wang, L. Ma, S.J. Gao, C.Z. Guo, K.N. Yao, L. Sheng, The Effect of Spatial Mode Distribution on Coupling Efficiency of Single-Mode Fiber: Theoretical Analysis and Experimental Verification, *Appl. Sci.-Basel* 9 (2019).
- [23] C. Zhai, Turbulence spectrum model and fiber-coupling efficiency in the anisotropic non-Kolmogorov satellite-to-ground downlink, *Results Phys.* 29 (2021) 104685, <https://doi.org/10.1016/j.rinp.2021.104685>.
- [24] L.B. Zhong, Y. Tian, C.H. Rao, Speckle transfer function for partial correction adaptive optics image reconstruction, *Opt. Lett.* 39 (2014) 4599–4602.
- [25] H. Ma, H. Liu, J. Zhang, P. Zhang, Numerical comparison of adaptive optics correction based on stochastic parallel gradient descent and phase conjugate in scintillation conditions, *Optik* 208 (2020) 164528, <https://doi.org/10.1016/j.ijleo.2020.164528>.